Asian Journal of Chemistry; Vol. 30, No. 7 (2018), 1593-1598

ASIAN JOURNAL OF CHEMISTRY

https://doi.org/10.14233/ajchem.2018.21266

Synthesis, Vibrational Spectroscopy, Crystal Structure and Hirshfeld Surface Analysis of Sodium Aquadichlororido[*N*-(3-aminopropyl)-*N*′-(propyl)ethane-1,2-diamine]chromium(III) Tetrachloridozincate

DOHYUN MOON[1] and JONG-HA CHOI[2,*]

[1]Pohang Accelerator Laboratory, POSTECH, Pohang 37673, Republic of Korea
[2]Department of Chemistry, Andong National University, Andong 36729, Republic of Korea

*Corresponding author: E-mail: jhchoi@anu.ac.kr

Received: 3 February 2018; *Accepted*: 6 March 2018; *Published online*: 31 May 2018; AJC-18937

The structure of aquadichlororido[*N*-(3-aminopropyl)-*N*′-(propyl)ethane-1,2-diamine]chromium(III) tetrachloridozincate, $Na[CrCl_2(C_8H_{21}N_3)(OH_2)]ZnCl_4$ ($C_8H_{21}N_3$ is *N*-(3-aminopropyl)-*N*′-(propyl)ethane-1,2-diamine), has been determined from synchrotron X-ray diffraction data. The complex crystallized in the space group $P2_1/n$ of the monoclinic system with four mononuclear formula units in a cell of dimensions a = 12.665(3), b = 14.048(3), c = 12.814(3) Å and β = 118.57(3)°. The Cr(III) ion is coordinated by three N atoms from the *N*-(3-aminopropyl)-*N*'-(propyl)ethane-1,2-diamine, two chloride ions and one O atom from a water molecule in a *trans*-meridional arrangement, displaying a slightly distorted octahedral geometry. Three Cr–N bond lengths are in the ranges 2.056 (2) to 2.126 (2) Å while the mean Cr–Cl and Cr–(OH_2) bond lengths are 2.3248 (8) and 2.0185 (17) Å, respectively. The crystal packing is stabilized by hydrogen bonding interactions among the amine N–H groups, the water molecule O–H group, Cl ligand and Cl atom of tetrachloridozincate anion. The tetrahedral $[ZnCl_4]^{2-}$ anion is distorted owing to its involvements in O–H···Cl and N–H···Cl hydrogen bonds and connecting Na^+ ion. Hirshfeld surface (HS) analysis by 3D molecular surface contours and 2D fingerprint plots have been used to analyze intermolecular interactions present in the crystal. The IR and Raman spectral properties are also described.

Keywords: Crystal structure, *N*-(3-Aminopropyl)-*N*'-(propyl)ethane-1,2-diamine, Chromium(III), Hirshfeld surface analysis.

INTRODUCTION

Geometric isomerism of coordination compounds formed by flexible polyamine three N donor ligands is an interesting field because these ligands can coordinate to metal ion facially or meridionally [1,2]. The syntheses and crystal structural analyses of cobalt(III) and chromium(III) complexes with the tridentate ligands, such as *N*-(2-aminoethyl)ethane-1,2-diamine (dien or 2,2-tri), *N*-(2-aminoethyl)propane-1,3-diamine (2,3-tri) and *N*-(3-aminopropyl)propane-1,3-diamine (dpt or 3,3-tri) have been studied extensively [3-6]. *N*-(3-aminopropyl)-*N*′-(propyl)ethane-1,2-diamine (**Scheme-I**) is also a tridentate polyamine ligand that can form a fused five and six- membered chelate ring system on coordination with a transition metal ion. However, transition metal containing the tridentate ligand have not received an attention until now. In this paper, we report on the preparation of a new complex, $Na[CrCl_2(C_8H_{21}N_3)(OH_2)]ZnCl_4$, (**Scheme-I**), vibrational spectral properties and its structural characterization by synchrotron single-crystal X-ray diffraction. A search of the Cambridge Structural Database (Version 5.38, May 2017 with 3 updates) [7] did not show any related metal complexes containing an

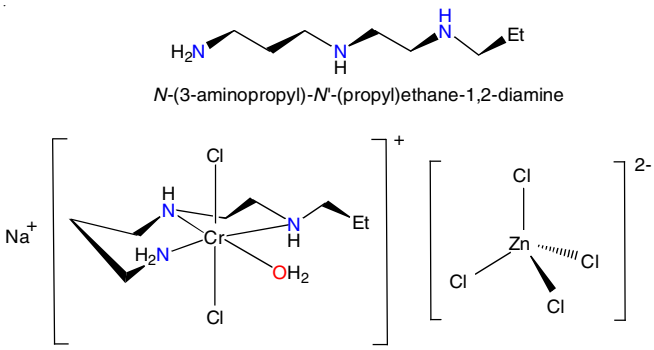

Scheme-I: Chemical structures of *N*-(3-aminopropyl)-*N*′-(propyl)ethane-1,2-diamine) and $Na[CrCl_2(C_8H_{21}N_3)(OH_2)]ZnCl_4$

N-(3-aminopropyl)-*N*′-(propyl)ethane-1,2-diamine ($C_8H_{21}N_3$). As far as we know, the title compound is the first metal complex with this typed tridentate ligand.

EXPERIMENTAL

Synthesis and measurements: All the chemicals were reagent grade materials and used without further purification. As starting material, *trans*-$[CrF(OH_2)(3,2,3\text{-tet})](ClO_4)_2{\cdot}H_2O$

(3,2,3-tet = *N*,*N*′-*bis*(3-aminopropyl)ethane-1,2-diamine), was prepared as described [8]. The crude perchlorate salt (0.2 g) was dissolved in 10 mL water at 333 K. The 10 mL solution of 0.5 M HCl containing 0.1 g of NaCl and 0.3 g of $ZnCl_2$ was gradually added. The unreacted materials were removed by filtration and allowed to stand at room temperature for a few days to give brown crystals of $Na[CrCl_2(C_8H_{21}N_3)(OH_2)]ZnCl_4$ suitable for synchrotron X-ray structural analysis. The mid-infrared spectrum was obtained from KBr pellets with a JASCO 460 plus series FT-IR spectrometer. Raman spectra was recorded on a Thermo Scientific DXR Confocal Raman microscope with a 532 nm laser excitation kit.

X-ray structural determination: A block brown crystal of the title compound was coated with parabar 10312 oil to prevent loss of crystallinity upon exposure to air. The diffraction data were measured on an ADSC Quantum-210 detector at BL2D-SMC with a silicon (111) double-crystal monochromator (0.62998 Å) at Pohang Accelerator Laboratory, Korea using synchrotron radiation and a nitrogen cold stream. The PAL BL2D-SMDC program [9] was used for data collection and HKL3000sm (Ver. 715) [10] was used for cell refinement, reduction and absorption correction. The structure was solved by the direct method with SHELXT-2015 program [11] and refined by full-matrix least-squares calculations with SHELXL -2015 program [11]. Molecular graphics were produced using DIAMOND-3 [12]. Crystal data, data collection and structure refinement details are summarized in Table-1. All H atoms were placed in geometrically idealized positions and constrained to ride on their parent atoms, with C–H distances of 0.96–0.97 Å and an N–H distance of 0.89-0.98 Å. All displacement parameters of H atoms $U_{iso}(H)$ were set to 1.2 or 1.5 U_{eq} of their respective parent atoms. The H atoms of coordinated water molecules were located from difference Fourier maps and refined with restraints and an O–H distance of 0.84 (1) Å, with $U_{iso}(H)$ values of 1.2 U_{eq}(O1A).

TABLE-1
CRYSTALLOGRAPHIC DATA FOR $Na[CrCl_2(C_8H_{21}N_3)(OH_2)]ZnCl_4$

Crystal data	
Chemical formula	$Na[CrCl_2(C_8H_{21}N_3)(OH_2)][ZnCl_4]$
M_r	530.35
Crystal system, space group	Monoclinic, $P2_1/n$
Temperature (K)	295
a, b, c (Å)	12.665 (3), 14.083 (3), 12.814 (3)
β (°)	118.57 (3)
V (Å^3)	2007.2 (9)
Z	4
Radiation type	Synchrotron, λ = 0.62998 Å
μ (mm^{-1})	1.67
Crystal size (mm)	0.10 × 0.07 × 0.04
Data collection	
Diffractometer	ADSC Q210 CCD area detector diffractometer
Absorption correction	Empirical (using intensity measurements) (HKL3000sm SCALEPACK)
T_{min}, T_{max}	0.881, 1.000
No. of measured, independent and observed [I > 2σ(I)] reflections	20252, 5372, 4588
R_{int}	0.026
$(\sin\theta/\lambda)_{max}$ (Å^{-1})	0.693
Refinement	
R[F^2 > 2σ(F^2)], wR(F^2), S	0.037, 0.113, 1.09
No. of reflections	5372
No. of parameters	198
No. of restraints	3
H-atom treatment	H atoms treated by a mixture of independent and constrained refinement
$\Delta\rho_{max}$, $\Delta\rho_{min}$ (e Å^{-3})	0.91, –0.95

RESULTS AND DISCUSSION

IR and Raman spectroscopy can be used to determine the configuration of isomers of transition metal complexes. The IR and Raman spectra of *trans* or *fac* isomer revealed a simpler pattern than that of *cis* or *mer* isomer and this pattern may be rationalized on the basis of the higher symmetry of *trans* or *fac* isomer [1,13-20]. The FT-IR and Raman spectra of the title complex are shown in Figs. 1 and 2, respectively. The resulting wavenumbers, intensities and assignments of the principal IR and Raman bands are also summarized in Table-2. The tentative assignments were made according to the literature data [13-21]. Two absorption peaks at 3483 and 3384 cm^{-1} and near 1632 cm^{-1} in the IR spectrum are due to the ν(O–H) stretching and δ(H–O–H) bending modes of water molecule. The absorptions at 3250–3050 cm^{-1} and 2970–2850 cm^{-1} (IR and Raman) are assigned to N–H and C–H stretching modes, respectively. Then, the IR band near 3200 cm^{-1} has been split into two components at 3239 and 3207 cm^{-1}, is assigned to NH_2 asymmetric stretching modes, while two bands at 3135 and 3070 cm^{-1} are assigned to NH_2 symmetric ones. The bands of moderate intensity observed at 2969 and 2936 cm^{-1}, are attributed to CH_2 asymmetric stretching mode and the bands at 2904 and 2881 cm^{-1} are assigned to symmetric stretching mode. These stretching modes are observed in the Raman spectrum at 3227, 3208 and 2969 cm^{-1}. The two strong IR absorption bands at 1595 and 1578 cm^{-1} and the Raman band at 1575 cm^{-1} can be assigned to NH_2 and CH_2 bending modes. The intense CH_2 bending deformation peaks are observed at 1462 and 1448 cm^{-1} (IR) and 1453 cm^{-1} (Raman). Medium to weak absorptions in the region of 1330-1290 cm^{-1} can be assigned to the symmetric NH_2 deformation. The three strong IR absorptions at 1059, 1007 and 997 cm^{-1} appear in the CH_2 twisting region. The medium peak at 874 cm^{-1}

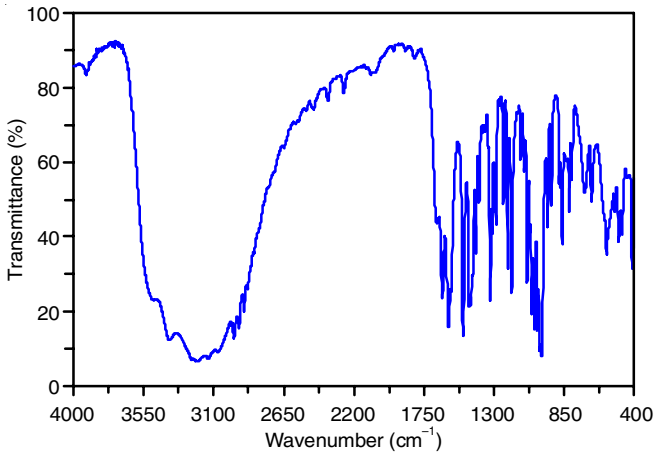

Fig. 1. FT-IR spectrum of $Na[CrCl_2(C_8H_{21}N_3)(OH_2)]ZnCl_4$

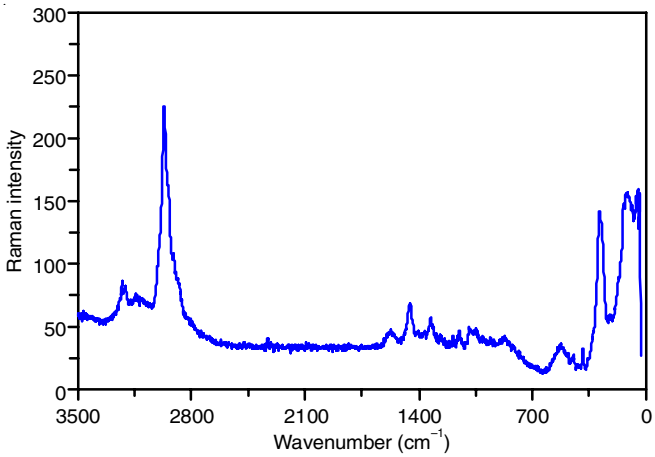

Fig. 2. Raman spectrum of Na[$CrCl_2(C_8H_{21}N_3)(OH_2)$]$ZnCl_4$

TABLE-2
ASSIGNMENTS OF THE SELECTED BANDS OCCURRING IN THE IR and RAMAN SPECTRA OF Na[$CrCl_2(C_8H_{21}N_3)(OH_2)$]$ZnCl_4$

IR bands (cm^{-1})	Raman bands (cm^{-1})	Assignments
3483 s, 3384 vs		ν(O–H)
3239 vs, 3207 s	3227 m, 3208 m	ν_a(N–H)
3135 s, 3073 s		ν_s(N–H)
2969 s, 2936 s	2969 vs	ν_a(C–H)
2904 s, 2881 m		ν_s(C–H)
2840-2260 w		Non-fundamental modes
1632 vs		δ(H_2O)
1595 vs, 1578 m	1575 m	δ(NH_2) scissoring
1500 vs,		
1462 vs, 1448 vs	1453 s	δ(CH_2) scissoring
1324 vs, 1311 m	1328 m	ω(CH_2) wagging
1297 m, 1286 vs		ω(CH_2) wagging
1239 s		ν(C–N)
1210 vs, 1189 vs	1151 m	ν(C–C)
1130 m, 1107 m		
1088 vs	1087 m	
1059 vs, 1039 vs	1049 m	τ(CH_2) twisting
1021 vs		ρ(NH_3)
1007 vs, 997 vs		ν_a(C–N)
959 s, 933 s		
882 m	876 m	ν_s(C–N)
863 vs		ρ(NH_2) rocking
817 s, 801 m		ρ(CH_2) rocking
721 m, 677 m		
579 vs, 501 m	526 m	δ(CCN)
480 m, 412 s	446 w	ν(Cr–N)
	392 m	ν(Cr–Cl)
	282 vs	ν(Zn–Cl)
	117 s, 87 m	δ($ZnCl_4$)

with two adjacent weak bands at 882 cm^{-1} are assigned to the NH_2 rocking vibration, while the two IR absorptions at 801 and 817 are due to CH_2 rocking vibration. The absorption positions of bending (δ), wagging (ω), twisting (τ) and rocking (ρ) bands of NH_2 and CH_2 deformations are not significantly affected by differing counter anions. The two peaks at 480 and 412 cm^{-1} can be assigned to the Cr–N stretching modes, whereas the Raman band at 392 cm^{-1} is assignable to the Cr–Cl stretching mode. The $[ZnCl_4]^{2-}$ entity contains five atoms and has nine fundamental vibrations. The point group derives from T_d for which there are four vibrations with symmetries: $\Gamma_{vib} = A_1 + E + 2T_2$. The strong band observed at 282 cm^{-1} in Raman spectrum is due to the Zn–Cl stretching mode of the $[ZnCl_4]^{2-}$ tetrahedron. The bands observed between 117 and 87 cm^{-1} are related to the $\nu_4(T_2)$ and $\nu_2(E)$ bending modes of the $[ZnCl_4]^{2-}$ tetrahedron, which involve the symmetric and asymmetric bending mode of the Cl–Zn–Cl bonds. The DFT B3LYP/3-21G calculated frequencies for $\nu_1(A_1)$, $\nu_2(E)$, $\nu_3(T_2)$ and $\nu_4(T_2)$ vibrational modes of $[ZnCl_4]^{2-}$ are 262, 79, 282 and 127 cm^{-1}, respectively [21]. The difference between the observed and calculated frequencies for the modes may be attributed to the perturbation by its crystal environment.

Crystallographic structure: The title complex crystallizes in the space group $P2_1/n$ of the monoclinic system with four mononuclear formula units in a cell of dimensions a = 12.665(3), b = 14.048(3), c = 12.814(3) Å and β = 118.57(3)°. Fig. 3 shows an ellipsoid plot of Na[$CrCl_2(C_8H_{21}N_3)(OH_2)$][$ZnCl_4$], with the atom numbering scheme. The asymmetric unit of the title compound contains discrete one cationic Cr(III) complex, one Na^+ cation and one $[ZnCl_4]^{2-}$ anion. In the chromium(III) complex cation, the three N atoms of *N*-(3-aminopropyl)-*N'*-(propyl)ethane-1,2-diamine, one water molecule and two chlorine atoms coordinate to the Cr metal center in a meridional arrangement for the tridentate ligand. In addition to, the two Cl ligands occupy the axial sites in a *trans*-configuration.

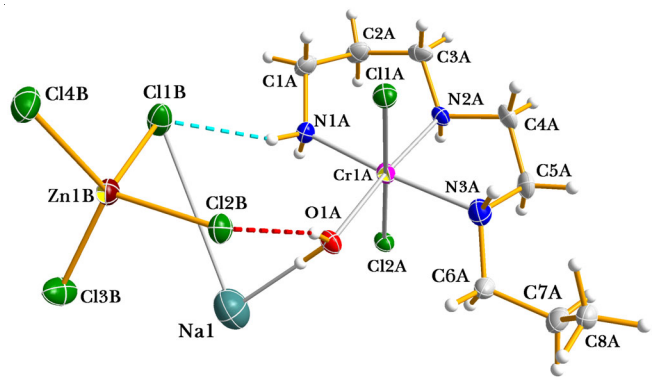

Fig. 3. Molecular structure of Na[$CrCl_2(C_8H_{21}N_3)(OH_2)$]$ZnCl_4$ drawn with 30 % probability displacement ellipsoids. Hydrogen-bonding interactions are indicated by dashed lines.

The Cr–N bond lengths for three amine nitrogens are in the range of 2.056 (2) to 2.126 (2) Å, in good agreement with those observed in *mer*-[Cr(dien)$_2$][$HgCl_4$]Cl(dmso)$_2$ [6], *mer*-[Cr(glygly)(dpt)]$ClO_4 \cdot H_2O$ (H_2glygly = glycylglycine) [2], *trans*-[CrF_2(2,2,3-tet)]ClO_4 (2,2,3-tet = *N*-(2-aminoethyl)-*N*2-(3-aminopropyl)ethane-1,2-diamine), *cis*-β-[Cr(N_3)$_2$(2,2,3-tet)]Br [22]. The Cr–Cl distances averaging 2.3248 (8) Å are close to the values found in *trans*-[$CrCl_2$(2,3,2-tet)]ClO_4 (2,3,2-tet = *N,N'-bis*(2-aminoethyl)propane-l,3-diamine) [23] and *cis*-β-[$CrCl_2$(2,2,3-tet)]ClO_4 [24]. The Cr1A–N1A and Cr1A–N3A bond lengths to the primary amines are slightly longer than the Cr1A–N2A bond length to the secondary amine. It is interesting to note that the Cr–N bond lengths to the primary amines in *cis*-β-[$CrCl_2$(2,3,2-tet)]ClO_4 [24] are slightly shorter than those to the secondary amines. The five-membered and six-membered chelate rings in the complex cation adopt stable *gauche* and chair conformations, respectively. The bond angles

of the five- and six-membered chelate rings around the chromium(III) atom are 83.46 (8) and 91.68 (8)°, respectively. The other N–C and C–C bond distances and Cr–N–C, N–C–C and C–C–C angles are typical in *gauche* and chair conformations. The sodium cation and $[ZnCl_4]^{2-}$ anion remain outside the coordination sphere. The Zn(II) atom in the complex anion exhibits a distorted tetrahedral geometry caused by the influence of hydrogen bonding and connecting Na^+ cation on the Zn–Cl bond lengths and the Cl–Zn–Cl angles. The Zn–Cl bond lengths range from 2.2198 (9) to 2.3142 (10) Å and the Cl–Zn–Cl angles from 102.85 (4) – 121.74 (4)°. The Cl3B and Cl4B atoms of $[ZnCl_4]^{2-}$ and Cl1A ligand are not involved in hydrogen bond and any considerable contact with other neighboring atoms in the crystal (Table-3).

TABLE-3
SELECTED BOND DISTANCES (Å) AND ANGLES (°) FOR $Na[CrCl_2(C_8H_{21}N_3)(OH_2)]ZnCl_4$

Cr1A-O1A	2.0185 (17)	N3A-C5A	1.488 (3)
Cr1A-N2A	2.0563 (18)	C1A-C2A	1.507 (4)
Cr1A-N1A	2.061 (2)	C2A-C3A	1.524 (4)
Cr1A-N3A	2.126 (2)	C4A-C5A	1.512 (4)
Cr1A-Cl1A	2.3121 (8)	C6A-C7A	1.521 (3)
Cr1A-Cl2A	2.3375 (7)	C7A-C8A	1.486 (4)
N1A-C1A	1.485 (3)	Zn1B-Cl3B	2.2198 (9)
N2A-C3A	1.482 (3)	Zn1B-Cl4B	2.2266 (8)
N2A-C4A	1.490 (3)	Zn1B-Cl1B	2.3073 (8)
N3A-C6A	1.483 (3)	Zn1B-Cl2B	2.3142 (10)
O1A-Cr1A-N2A	175.49 (8)	C4A-N2A-Cr1A	108.23 (15)
O1A-Cr1A-N1A	91.91 (8)	C6A-N3A-C5A	113.8 (2)
N2A-Cr1A-N1A	91.68 (8)	C6A-N3A-Cr1A	116.43 (14)
O1A-Cr1A-N3A	92.98 (8)	C5A-N3A-Cr1A	107.00 (15)
N2A-Cr1A-N3A	83.46 (8)	N1A-C1A-C2A	111.6 (2)
N1A-Cr1A-N3A	175.10 (8)	C1A-C2A-C3A	113.8 (2)
O1A-Cr1A-Cl1A	89.08 (6)	N2A-C3A-C2A	112.5 (2)
N2A-Cr1A-Cl1A	93.59 (6)	N2A-C4A-C5A	108.69 (19)
N1A-Cr1A-Cl1A	91.07 (7)	N3A-C5A-C4A	108.3 (2)
N3A-Cr1A-Cl1A	88.66 (6)	N3A-C6A-C7A	116.2 (2)
O1A-Cr1A-Cl2A	87.88 (6)	C8A-C7A-C6A	113.3 (2)
N2A-Cr1A-Cl2A	89.42 (6)	Cl3B-Zn1B-Cl4B	121.74 (4)
N3A-Cr1A-Cl2A	91.11 (6)	Cl3B-Zn1B-Cl1B	110.83 (4)
Cl1A-Cr1A-Cl2A	176.93 (3)	Cl4B-Zn1B-Cl1B	102.85 (4)
C1A-N1A-Cr1A	119.86 (16)	Cl3B-Zn1B-Cl2B	109.37 (4)
C3A-N2A-C4A	111.0 (2)	Cl4B-Zn1B-Cl2B	107.44 (4)
C3A-N2A-Cr1A	118.87 (15)	Cl1B-Zn1B-Cl2B	102.89 (3)

Symmetry codes: (i) x–1/2, –y+1/2, z–1/2; (ii) –x+2, –y+1, –z+2; (iii) x+1/2, –y+1/2, z+1/2.

The cations and anions in the crystals are held together by hydrogen bonds (Table-4) between the NH or OH groups of the tridentate ligand and coordinating water molecule as donors, the Cl ligands and the Cl atoms of the tetrachloridozincate anion. The $[ZnCl_4]^{2-}$ anion and the water molecule are also connecting Na^+ ion. An array of these contacts generate a three dimensional network as shown in Fig. 4. The extensive contacts help to stabilize the crystal structure.

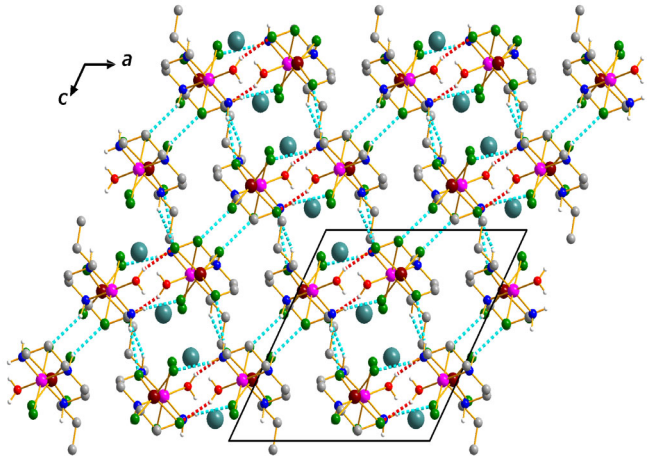

Fig. 4. Crystal packing of $Na[CrCl_2(C_8H_{21}N_3)(OH_2)]ZnCl_4$ as seen along the b direction. Dashed lines represent O–H···Cl (red) and N–H···Cl (cyan) hydrogen bonds, respectively

Hirshfeld surface analysis: Visualization and exploration of intermolecular close contacts of a structure is invaluable and this can be achieved using the Hirshfeld (HS) [25]. The Hirshfeld is a useful tool for describing the surface characteristics of the molecules. The analysis has been performed by using CrystalExplorer17 [26]. The molecular HS d_{norm} surface, shape index and curvedness are shown in Fig. 5.

The d_{norm} surface is used for identification of very close intermolecular interactions while the shape index is most sensitive to very subtle changes in surface shape. The curvedness is the measurement of how much shape, the flat areas of the surface correspond to low values of curvedness, while sharp curvature areas correspond to high values of curvedness and usually tend to divide the surface into patches, indicating interactions between neighboring molecules. The d_{norm} surface shows the red and white spots indicating main contacts due to H···Cl, H···H and H···N interactions. The 2-D fingerprint plots complement the HS, quantitatively summarizing the nature and type of intermolecular contacts experienced by molecules in the crystal. 2-D fingerprint plot [27] of various interactions is shown in Fig. 6, where d_i is the closet internal distance from a given point on the HS and d_e is the closest external contact, respectively [27-29].

The packing of the molecules is primarily driven by the H···Cl, H···H, H···N and N···Cl interactions. Apart from these above, H···Zn, N···Zn and Cl···Cl contacts have very little contributions of 0.3, 0.2 and 0.2 %, respectively. The relative intermolecular interactions are summarized in Fig. 7.

TABLE-4
HYDROGEN BOND PARAMETERS (Å,°) FOR $Na[CrCl_2(C_8H_{21}N_3)(OH_2)]ZnCl_4$

D–H···A	D–H	H···A	D···A	D–H···A
O1A–H1O1···Cl2B	0.836 (10)	2.276 (15)	3.0653 (19)	158 (3)
N1A–H1A1···Cl3B^{i}	0.89	2.54	3.317(3)	146.4
N1A–H1A2···Cl1B	0.89	2.40	3.242(2)	158.4
N2A–H2A···Cl2A^{ii}	0.98	2.60	3.413(2)	139.8
N3A–H3A···Cl2B^{iii}	0.98	2.44	3.320(2)	148.5

Symmetry codes: (i) –x+2, –y+1, –z+2; (ii) –x+1, –y+1, –z+2; (iii) –x+1, –y+1, –z+1.

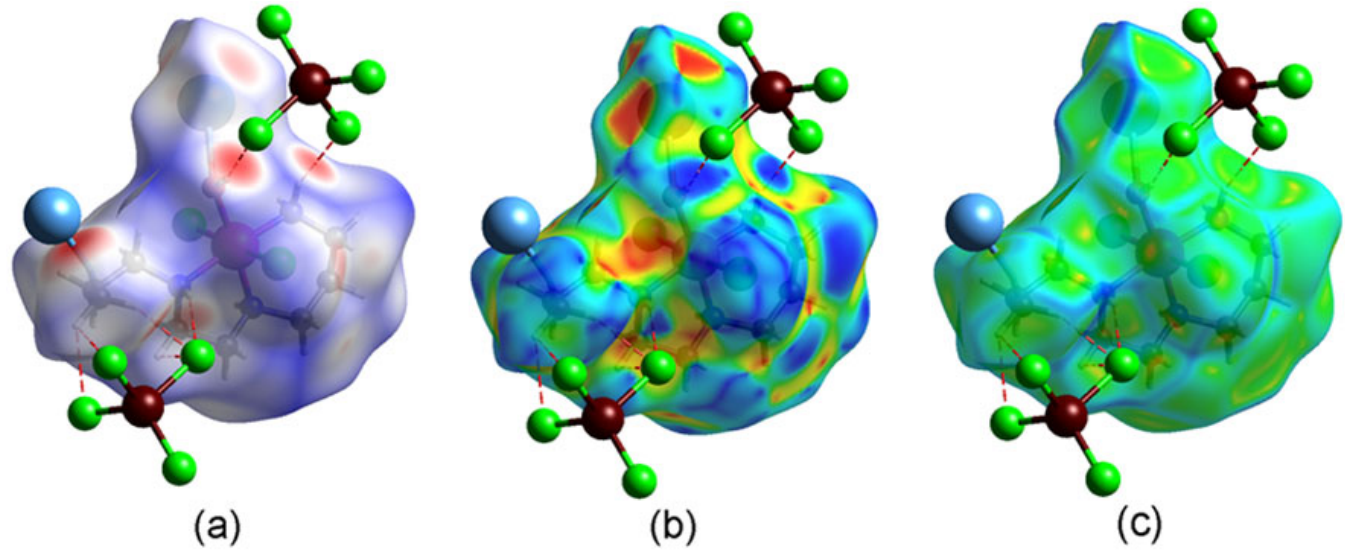

Fig. 5. Hirshfeld surfaces mapped with (a) d_{norm}, (b) shape-index and (c) curvedness

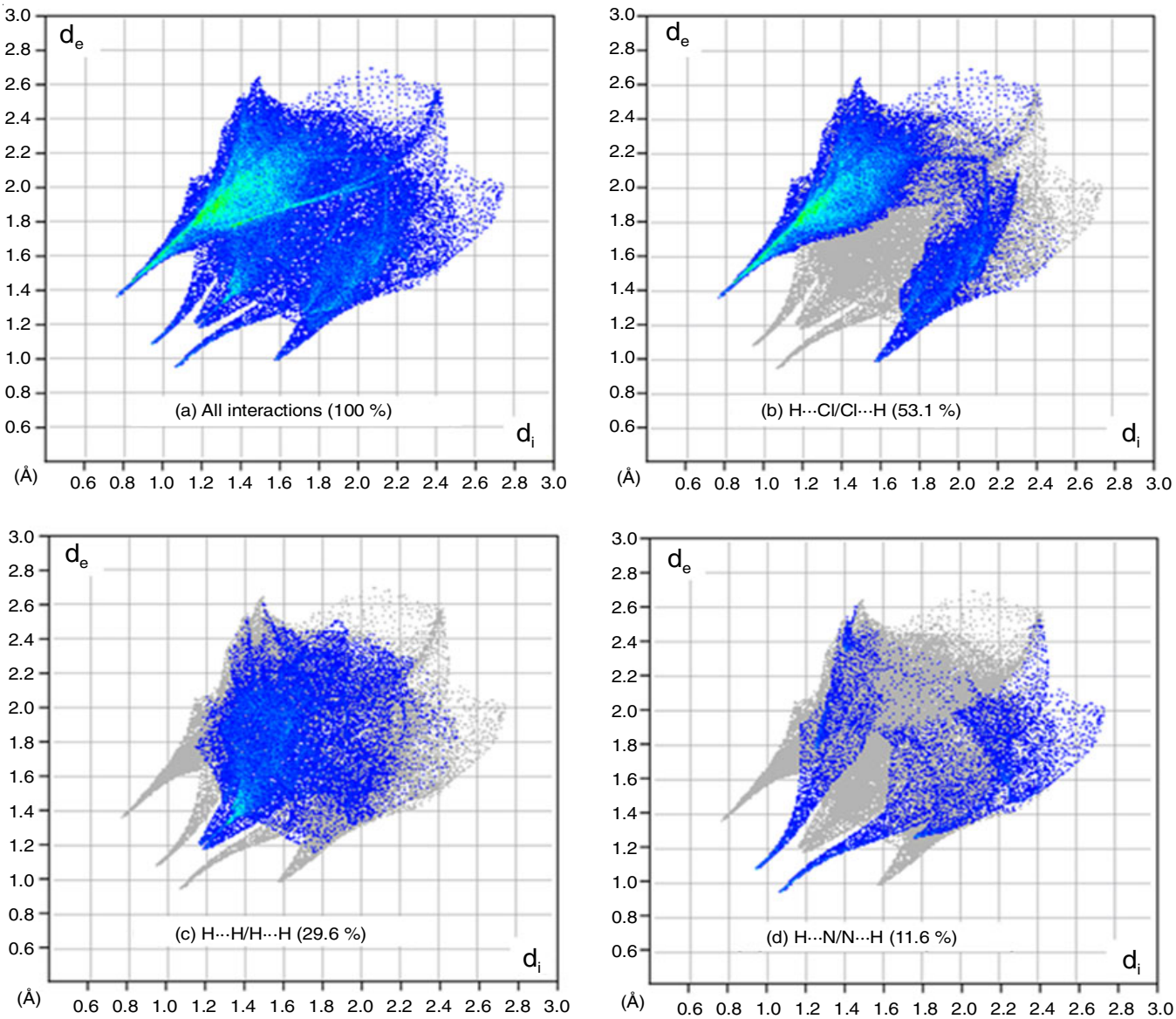

Fig. 6. Two-dimensional fingerprint plots of $Na[CrCl_2(C_8H_{21}N_3)(OH_2)]ZnCl_4$ showing (a) all interactions and delineated into (b) H···Cl, (c) H···H and (d) H···N interactions

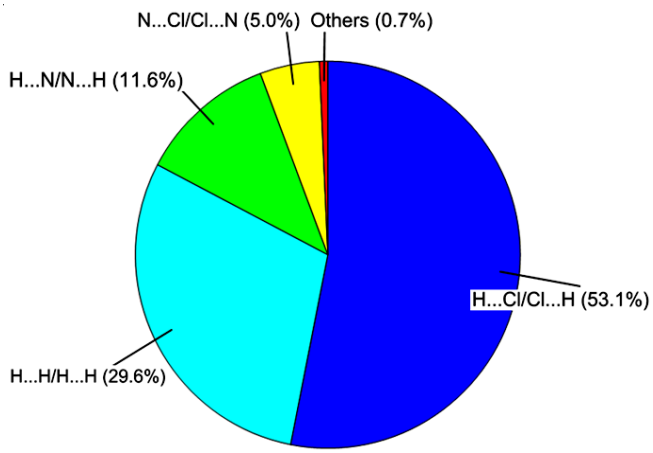

Fig. 7. Percentage contribution of individual intermolecular interactions to the Hirshfeld surfaces of $Na[CrCl_2(C_8H_{21}N_3)(OH_2)]ZnCl_4$

Conclusion

A new mixed ligand chromium(III) complex, $Na[CrCl_2(C_8H_{21}N_3)(OH_2)]ZnCl_4$ has been synthesized and characterized by IR, Raman, single-crystal X-ray diffraction and HS analyses. It is suggested that the Cr(III) ion in the title complex was coordinated to three N atoms from the *N*-(3-aminopropyl)-*N'*-(propyl)ethane-1,2-diamine, two chloride ions and one O atom from a water molecule in a *trans*-meridional arrangement, displaying a slightly distorted octahedral geometry. Three Cr–N bond lengths were in the ranges 2.056 (2) to 2.126 (2)Å while the mean Cr–Cl and Cr–(OH_2) bond lengths of 2.3248 (8) and 2.0185 (17)Å were observed. HS analysis with 2D fingerprint plots showed that the H···Cl, H···H, H···N and N···Cl interactions are the main intermolecular interactions. The crystal packing is stabilized by hydrogen bonding interactions among the amine N–H groups, the water molecule O–H group, Cl ligand and Cl atom of tetrachloridozincate anion. The tetrahedral $[ZnCl_4]^{2-}$ anion is distorted owing to its involvements in O–H···Cl and N–H···Cl hydrogen bonds and connecting Na^+ ion.

Suppelementary material: Crystallographic data for the structures reported here have been deposited with CCDC Deposition No 1821783. These data can be obtained free of charge from the Cambridge Crystallographic Data Centre, 12 Union Road, Cambridge CB2 1EZ, UK, Fax: +441223336033; E-mail: deposit@ccdc.cam.ac.uk.

ACKNOWLEDGEMENTS

This work was supported by a Research Grant of Andong National University. The X-ray crystallography experiment at PLS-II BL2D-SMC beamline was supported in part by MSIT and POSTECH.

REFERENCES

1. J.-H. Choi and P.E. Hoggard, *Polyhedron*, **11**, 2399 (1992); https://doi.org/10.1016/S0277-5387(00)83531-7.
2. J.-H. Choi, I.H. Suh and S.H. Kwak, *Acta Crystallogr. C*, **51**, 1745 (1995); https://doi.org/10.1107/S0108270195002800.
3. T.W. Hambley, G.H. Searle and M.R. Snow, *Aust. J. Chem.*, **35**, 1285 (1982); https://doi.org/10.1071/CH9821285.
4. D.A. House, *Inorg. Chim. Acta*, **121**, 167 (1986); https://doi.org/10.1016/S0020-1693(00)84516-8.
5. D.A. House and W.T. Robinson, *Inorg. Chim. Acta*, **141**, 211 (1988); https://doi.org/10.1016/S0020-1693(00)83912-2.
6. D.A. House, V. McKee and W.T. Robinson, *Inorg. Chim. Acta*, **157**, 15 (1989); https://doi.org/10.1016/S0020-1693(00)83418-0.
7. C.R. Groom, I.J. Bruno, M.P. Lightfoot and S.C. Ward, *Acta Crystallogr. B*, **72**, 171 (2016); https://doi.org/10.1107/S2052520616003954.
8. J.-H. Choi and U. Lee, *Acta Crystallogr. E Struct. Rep. Online*, **64**, m1186 (2008); https://doi.org/10.1107/S1600536808026081.
9. J.W. Shin, K. Eom and D. Moon, *J. Synchrotron Rad.*, **23**, 369 (2016); https://doi.org/10.1107/S1600577515021633.
10. Z. Otwinowski and W. Minor, eds., C.W. Carter Jr. and R.M. Sweet, Methods in Enzymology, Academic Press, New York, Vol. 276, Macromolecular Crystallography, Part A, pp. 307-326 (1997).
11. G.M. Sheldrick, *Acta Crystallogr. A*, **71**, 3 (2015); https://doi.org/10.1107/S2053273314026370.
12. K. Brandenburg and H. Putz, DIAMOND-3, University of Bonn, Germany (2014).
13. D. Moon and J.-H. Choi, *Spectrochim. Acta A*, **138**, 774 (2015); https://doi.org/10.1016/j.saa.2014.11.099.
14. J.-H. Choi, *Chem. Phys.*, **256**, 29 (2000); https://doi.org/10.1016/S0301-0104(00)00097-5.
15. J.-H. Choi, *Spectrochim. Acta A*, **56**, 1653 (2000); https://doi.org/10.1016/S1386-1425(00)00221-3.
16. J.-H. Choi, I.G. Oh, T. Suzuki and S. Kaizaki, *J. Mol. Struct.*, **694**, 39 (2004); https://doi.org/10.1016/j.molstruc.2004.01.034.
17. J.-H. Choi, Y.P. Hong and Y.C. Park, *Spectrochim. Acta A*, **58**, 1599 (2002); https://doi.org/10.1016/S1386-1425(01)00611-4.
18. J.-H. Choi and S.H. Lee, *J. Mol. Struct.*, **932**, 84 (2009); https://doi.org/10.1016/j.molstruc.2009.05.048.
19. J.-H. Choi, *Inorg. Chim. Acta*, **362**, 4231 (2009); https://doi.org/10.1016/j.ica.2009.05.024.
20. J.-H. Choi and D. Moon, *J. Mol. Struct.*, **1059**, 325 (2014); https://doi.org/10.1016/j.molstruc.2013.12.008.
21. K. Karoui, M. Ben Bechir, A. Ben Rhaiem, A. Bulou, F. Calvayrac and K. Guidara, *Phase Transit.*, **87**, 613 (2014); https://doi.org/10.1080/01411594.2013.879588.
22. J.-H. Choi, W. Clegg and R.W. Harrington, *Z. Anorg. Allg. Chem.*, **637**, 562 (2011); https://doi.org/10.1002/zaac.201000375.
23. D. Moon and J.H. Choi, *Acta Crystallogr. E Struct. Rep. Online*, **72**, 424 (2016); https://doi.org/10.1107/S2056989016002978.
24. J.-H. Choi, H.-S. Kim and M.H. Habibi, *Bull. Korean Chem. Soc.*, **29**, 1399 (2008); https://doi.org/10.5012/bkcs.2008.29.7.1399.
25. M.A. Spackman and D. Jayatilaka, *CrystEngComm*, **11**, 19 (2009); https://doi.org/10.1039/B818330A.
26. M.J. Turner, J.J. McKinnon, S.K. Wolff, D.J. Grimwood, P.R. Spackman, D. Jayatilaka and M.A. Spackman, CrystalExplorer17, University of Western Australia (2017).
27. M.A. Spackman and J.J. McKinnon, *CrystEngComm*, **4**, 378 (2002); https://doi.org/10.1039/B203191B.
28. D. Moon, S. Tanaka, T. Akitsu and J.-H. Choi, *J. Mol. Struct.*, **1154**, 338 (2018); https://doi.org/10.1016/j.molstruc.2017.10.066.
29. T. Aree, Y.P. Hong and J.-H. Choi, *J. Mol. Struct.*, **1163**, 86 (2018); https://doi.org/10.1016/j.molstruc.2018.02.102.